

# Two-Dimensional Sine Chaotification System With Hardware Implementation

Zhongyun Hua<sup>1</sup>, Member, IEEE, Yicong Zhou<sup>2</sup>, Senior Member, IEEE, and Bocheng Bao<sup>1</sup>

**Abstract**—Chaotic systems are widely employed in many practical applications for their significant properties. Existing chaotic systems may suffer from the drawbacks of discontinuous chaotic ranges and frail chaotic behaviors. To solve this issue, this paper proposes a two-dimensional (2D) sine chaotification system (2D-SCS). 2D-SCS can not only significantly enhance the complexity of 2D chaotic maps, but also greatly extend their chaotic ranges. As examples, this paper applies 2D-SCS to two existing 2D chaotic maps to obtain two enhanced chaotic maps. Performance evaluations show that these two enhanced chaotic maps have robust chaotic behaviors in much larger chaotic ranges than existing 2D chaotic maps. A microcontroller-based experiment platform is also designed to implement these enhanced chaotic maps in hardware devices. Furthermore, to investigate the application of 2D-SCS, these two enhanced chaotic maps are applied to design a pseudorandom number generator. Experiment results show that these enhanced chaotic maps can produce better random sequences than the existing 2D and several state-of-the-art one-dimensional (1D) chaotic maps.

**Index Terms**—Chaotic system, chaotification, hardware implementation, nonlinear system, random number generator.

## I. INTRODUCTION

NONLINEAR system attracts increasing attention from various fields and has a wide body of researches in industrial applications [1]–[3]. For example, a class of uncertain cascaded

Manuscript received March 1, 2019; revised May 15, 2019; accepted May 31, 2019. Date of publication June 18, 2019; date of current version January 14, 2020. This work was supported in part by the National Key Research and Development Program of China under Grant 2018YFB1003805 and Grant 2016YFB0800804, in part by the Shenzhen Science and Technology Program under Grant JCYJ20170307150704051 and Grant JCYJ20170811160212033, in part by the National Natural Science Foundation of China under Grant 61701137, in part by the Macau Science and Technology Development Fund under Grant FDCT/189/2017/A3, and in part by the Research Committee at the University of Macau under Grant MYRG2016-00123-FST and Grant MYRG2018-00136-FST. Paper no. TII-19-0698. (Corresponding author: Zhongyun Hua.)

Z. Hua is with the School of Computer Science and Technology, Harbin Institute of Technology, Shenzhen, Shenzhen 518055, China (e-mail: huazhym@gmail.com; huazhongyun@hit.edu.cn).

Y. Zhou is with the Department of Computer and Information Science, University of Macau, Macau 999078, China (e-mail: yicongzhou@um.edu.mo).

B. Bao is with the School of Information Science and Engineering, Changzhou University, Changzhou 213164, China (e-mail: mervinbao@126.com).

Color versions of one or more of the figures in this paper are available online at <http://ieeexplore.ieee.org>.

Digital Object Identifier 10.1109/TII.2019.2923553

nonlinear systems was developed for motor-servo systems [4]. Chaos theory is a branch of nonlinear theory and it studies chaotic behaviors that are sensitive to initial conditions [5]–[7]. According to the definition of R. L. Devaney in [8], a dynamical system is considered to have chaotic behaviors if it is sensitive to initial conditions and topological mixing, and has dense periodic orbits. Thanks to these properties, chaotic systems have been studied and applied to many industrial applications [9]–[12]. Particularly, they are widely used in pseudorandom number generators [13], [14], because chaotic systems and pseudorandom number generators have the same properties of initial condition sensitivity and unpredictability [15].

A chaotic system is a mathematical model to simulate chaotic behaviors and many chaotic systems have been designed [16]. However, these chaotic systems may have some drawbacks in various aspects. First, their chaotic ranges are small or discontinuous [17]. When chaotic systems are simulated in finite-precision platforms, their control parameters can only approximate the real parameters, due to precision truncation. Thus, if the chaotic ranges are too small or discontinuous, the approximations of the control parameters may be within the non-chaotic ranges. This leads the chaotic systems to lose chaos properties [18]. Second, the trajectories of the existing chaotic systems may visit only a small region of their phase planes. This causes negative effects to many chaos-based applications. For example, the chaos-based pseudorandom number generators cannot produce uniformly distributed random sequences [13]. Besides, some existing chaotic systems have simple chaotic behaviors and their chaotic signals can be deduced using some technologies [19], [20]. Theoretically, the chaotic signals of a chaotic system are deterministic only when knowing the initial condition of the chaotic system. However, with simple chaotic behaviors, the chaotic signals of some chaotic systems can be directly estimated without knowing the initial conditions [21]. When this happens, the corresponding chaotic systems lose unpredictability, which leads to failures of some applications using chaos [22].

Recently, many research works have been devoted to overcoming the drawbacks of existing chaotic systems [23], [24]. Some research works focus on enhancing the complexity of chaotic signals. They either contaminate chaotic signals using some noise [25], [26] or replace fixed control parameters of chaotic systems using dynamical ones [27]. For example, Lan *et al.* introduced a parameter-selection method to remove the control parameters that result in weak chaotic behaviors [28]. By setting a predefined threshold, the control parameters with

large Kolmogrov entropy are selected to generate chaotic signals. This can obviously enhance the complexity of chaotic signals and have positive effects to some chaos-based applications [3]. However, it cannot change the complexity and behaviors of chaotic systems, and thus, may not be suitable for some applications such as nonlinear control and chaos synchronization [16], [29].

Another effective strategy of overcoming the drawbacks of existing chaotic systems is to enhance the dynamic complexity of chaotic systems [17], [30]. This strategy either enhances the complexity of existing chaotic systems or designs new chaotic systems with more complex behaviors [31]. Currently, this strategy focuses on one-dimensional (1D) chaotic systems. This is because 1D chaotic systems have simple structures that need low implementation costs [17]. However, the 1D chaotic systems may have disadvantages such as easily predicted chaotic signals. The high-dimensional chaotic systems, on the other hand, have complicated structures and their chaotic signals are difficult to predict. However, complicated structures also lead to expensive implementation costs. Thus, this paper focuses on enhancing the chaos complexity of two-dimensional (2D) chaotic systems since the 2D chaotic systems can balance the tradeoff between the implementation cost and chaotic performance.

To enhance the chaos complexity of 2D chaotic systems, this paper proposes a 2D sine chaotification system (2D-SCS). 2D-SCS uses the sine transform as a chaotification framework and applies it to each output of 2D chaotic systems. As the sine transform is a bounded function for any input, 2D-SCS can generate chaos in a large parameter range. Examples of enhanced chaotic maps and application verify the effectiveness of 2D-SCS. The main novelty and contributions of this paper are summarized as follows.

- 1) We propose 2D-SCS as a universal chaotification framework for enhancing chaos performance of 2D chaotic maps. 2D-SCS is not only able to significantly enhance the complexity of 2D chaotic maps, but also able to greatly extend their chaotic ranges.
- 2) To demonstrate the effectiveness of 2D-SCS, two existing 2D chaotic maps are enhanced by 2D-SCS. Performance evaluations show that these enhanced maps can achieve considerably larger chaotic ranges and more complex chaotic behaviors than the 2D chaotic maps before enhanced and some newly generated 1D chaotic maps.
- 3) A microcontroller-based experiment platform is developed to implement the enhanced chaotic maps of 2D-SCS in hardware devices. The results indicate that these enhanced chaotic maps have simple hardware implementations.
- 4) To further investigate the application of 2D-SCS, these enhanced chaotic maps are applied to the pseudorandom number generator. Experiment results show that these enhanced maps can generate more random sequences than the 2D chaotic maps before enhanced and some newly generated 1D chaotic maps.

The rest of this paper is organized as follows. Section II presents two existing 2D chaotic maps and reviews the related works as background. Section III presents the proposed

2D-SCS and studies two examples of the enhanced chaotic maps of 2D-SCS. Section IV evaluates the performance of the two enhanced chaotic maps. Section V implements these two enhanced chaotic maps in hardware devices and investigates their application in pseudorandom number generator. Finally, Section VI concludes this paper.

## II. PRELIMINARY KNOWLEDGE

This section presents two 2D chaotic maps, which are used as examples to demonstrate the effectiveness of 2D-SCS in Section III. The related works are also reviewed as a background.

### A. Existing 2D Chaotic Maps

The Hénon map was developed by Michel Hénon and it is one of the most studied examples of 2D chaotic systems [16]. The Hénon map is defined as

$$\begin{cases} x_{n+1} = 1 - ax_n^2 + y_n \\ y_{n+1} = bx_n \end{cases} \quad (1)$$

where  $a$  and  $b$  are two control parameters. The Hénon map can achieve excellent chaos dynamics when  $a = 1.4$  and  $b = 0.3$ .

The 2D sine logistic modulation (2D-SLM) map is a recently developed 2D chaotic system [32]. It is developed from the 1D sine and logistic maps. The mathematical equation of the 2D-SLM map is written as

$$\begin{cases} x_{n+1} = a(\sin(\pi y_n) + b)x_n(1 - x_n) \\ y_{n+1} = a(\sin(\pi x_{n+1}) + b)y_n(1 - y_n) \end{cases} . \quad (2)$$

The two control parameters  $a \in [0, 1]$  and  $b \in [0, 3]$ . The 2D-SLM map shows classical chaotic behaviors when  $a = 1$  and  $b = 3$ .

The bifurcation diagram of a chaotic system shows the visited or approached values of one variable with the change of control parameter(s), while the trajectory of a 2D chaotic system shows the visited or approached points in the 2D phase plane. Thus, bifurcation diagram and trajectory of a 2D chaotic system can visually display the behaviors of the system. Fig. 1 shows the bifurcation diagrams and trajectories of the Hénon and 2D-SLM maps. To better show the observation results, their bifurcation diagrams are plotted with the change of one parameter and another parameter is set as a fixed value that can make the two chaotic maps achieve complex chaotic behaviors. As can be seen, the Hénon and 2D-SLM maps have small chaotic ranges and their chaotic ranges are discontinuous. Meanwhile, their trajectories visit only a small region of the phase plane.

The Hénon and 2D-SLM maps have simple structures that can benefit their implementation costs. However, as shown in Fig. 1, they also have various disadvantages. First, their simple structures make their trajectories have some patterns and they cannot distribute uniformly in the phase plane. Second, they have small chaotic ranges, indicating that they have chaotic behaviors in only few parameter settings. Moreover, their chaotic ranges are discontinuous and even isolated. This means that their chaotic behaviors are frail and a small change to their control parameters may lead their parameters to enter

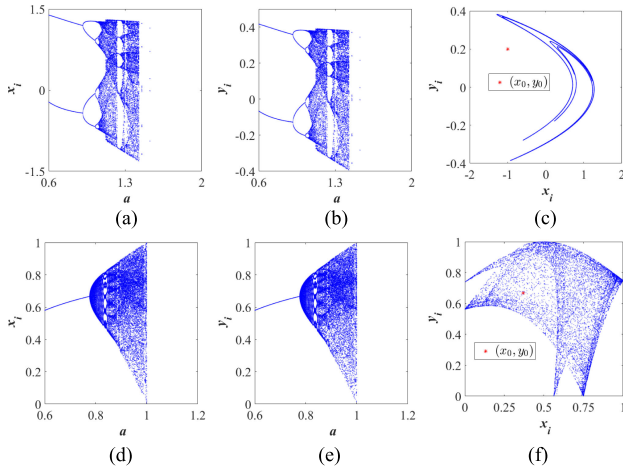


**Fig. 1.** Bifurcation diagrams and trajectories of two 2D chaotic maps. (a)-(b) Hénon map's two bifurcation diagrams under  $b = 0.3$  and  $a \in [0.6, 2]$  and (c) its trajectory under  $(a, b) = (1.4, 0.3)$ . (d)-(e) 2D-SLM map's two bifurcation diagrams under  $b = 1$  and  $a \in [0.6, 1.2]$  and (f) its trajectory under  $(a, b) = (1, 3)$ .

the nonchaotic ranges. This brings negative effects to some chaos-based applications, because the parameters of chaotic systems are easily perturbed by different kinds of noise when chaotic systems are simulated in practical applications [33].

### B. Related Works

One effective strategy of overcoming the drawbacks of existing chaotic maps is to develop new chaotic systems with complex behaviors. At present, some efforts have been devoted to addressing this and they can be classified into two categories [17], [34]–[37]. The first category of efforts designs new chaotic systems with specific mathematical definitions. In [35], Yu *et al.* developed a simple fourth-order double-torus chaotic circuit. Dynamical behavior investigation demonstrates that the chaotic circuit can generate complex chaotic attractors by switching and displacing a basic linear circuit. In [34], Chen *et al.* constructed a chaotic system by controlling a nominal system using a feedback controller. Theoretical analysis demonstrates that the constructed chaotic system has complex dynamic behaviors and is suitable for secure communication.

The second type of efforts is to design some general chaotic frameworks. Using these frameworks, one can obtain many new chaotic maps. In [17], Wu *et al.* proposed a wheel-switching chaotic framework. Using a controlling sequence to determine which chaotic map is selected, the chaotic framework is able to generate a large number of new chaotic sequences. In [37], Hua *et al.* introduced a parameter-control chaotic framework. This framework can produce a large number of new chaotic maps using the outputs of a chaotic map to dynamically control the parameter of another chaotic map. Nine examples of new chaotic maps are produced and evaluated. The results demonstrate that these generated chaotic maps have more complex chaotic behaviors than existing chaotic maps.

Compared with existing chaotic maps, these newly generated chaotic maps have more control parameters and more complex chaotic behaviors, and thus, can significantly promote the

chaos-based applications. However, these efforts still have some disadvantages. The chaotic maps generated using these previous works cannot achieve continuous chaotic ranges [35]–[37]. Besides, the outputs of these generated chaotic maps cannot uniformly distribute in the entire phase plane [17], [34]–[36].

### III. TWO-DIMENSIONAL SINE CHAOTIFICATION SYSTEM

This section introduces a 2D-SCS and studies two examples of the enhanced chaotic maps of 2D-SCS.

#### A. Two-Dimensional Sine Chaotification System

To address the drawbacks of existing chaotic maps in discontinuous chaotic ranges, frail chaotic behaviors, and incomplete output distributions, this study proposes the 2D-SCS to enhance the chaos complexity of existing 2D chaotic maps. 2D-SCS uses a sine transform as a chaotification framework and applies it to each output of existing 2D chaotic maps. The general form of 2D-SCS, denoted as  $\mathbf{S}(x, y)$ , can be represented as

$$\mathbf{S}(x, y) = \sin(\pi \mathbf{F}(x, y)) \quad (3)$$

where  $x$  and  $y$  are two variables, and  $\mathbf{F}(x, y)$  is an existing 2D chaotic map that can be represented as

$$\begin{cases} x_{n+1} = A(x_n, y_n) \\ y_{n+1} = B(x_n, y_n) \end{cases} .$$

Then, the iterative form of 2D-SCS in (3) can be written as

$$\begin{cases} x_{n+1} = \sin(\pi A(x_n, y_n)) \\ y_{n+1} = \sin(\pi B(x_n, y_n)) \end{cases} . \quad (4)$$

For many existing 2D chaotic maps, with the increment of their control parameters, their phase planes become uncompact. This makes their output values diverge to infinity. Thus, they cannot exhibit chaotic behaviors with the increment of their control parameters and have small chaotic ranges. The sine transform is a bounded function and its output range is  $[-1, 1]$  for any input. According to [37], the sine map with parameter equal to one can achieve complex nonlinear dynamics and its outputs can uniformly distribute in its phase plane. Thus, the sine transform is a natural candidate to enhance the complexity of chaotic maps. Then, 2D-SCS has the following properties: 1) it can significantly enhance the dynamic complexity of existing 2D chaotic maps in their chaotic ranges and 2) it is able to produce chaos in the parameters where existing chaotic maps do not have chaotic behaviors. This can greatly extend the chaotic ranges of existing maps.

As mentioned in Section II-B, chaotic maps generated by previous works cannot achieve continuous chaotic ranges, or their outputs cannot uniformly distribute in the entire phase plane, or neither. However, the enhanced chaotic maps of 2D-SCS can achieve robust chaotic behaviors in continuous chaotic ranges and their outputs can distribute in the full region of the phase plane. These properties are verified by performance evaluation results in Section IV. To show the effectiveness of 2D-SCS, as examples, the two existing chaotic maps presented

in Section II-A are enhanced by 2D-SCS and the chaotic behaviors of the enhanced chaotic maps are studied.

### B. Enhanced Hénon Map

**1) Definition:** When the Hénon map in (1) is used as the existing 2D chaotic map  $\mathbf{F}(x, y)$  in (3), the enhanced Hénon map can be obtained and it is defined as

$$\begin{cases} x_{n+1} = \sin(\pi(1 - \tilde{a}x_n^2 + y_n)) \\ y_{n+1} = \sin(\pi\tilde{b}x_n) \end{cases} \quad (5)$$

where the two control parameters  $\tilde{a}, \tilde{b} \in \mathbb{R}$ .

**2) Stability:** The stability of a dynamical system can be deduced using its fixed points. A fixed point of a dynamical system is an element of its domain that maps to itself. For example,  $\mathbf{v}$  is a fixed point of  $f(\cdot)$  if  $f(f(\cdots f(\mathbf{v}) \cdots)) = \mathbf{v}$ . The fixed points of the enhanced Hénon map, denoted as  $(\hat{x}, \hat{y})$ , are the solutions of the following 2D equation:

$$\begin{cases} \hat{x} = \sin(\pi(1 - \tilde{a}\hat{x}^2 + \hat{y})) \\ \hat{y} = \sin(\pi\tilde{b}\hat{x}) \end{cases} \quad . \quad (6)$$

The fixed points of a dynamical system may be stable or unstable. A stable fixed point indicates that the states approaching the fixed point will be attracted and the system will become stationary in the long-term evolution. An unstable fixed point indicates that the close states will be rejected by the fixed point and the system will oscillate. The gradient of a system can indicate the stability of the fixed points. A 2D dynamical system with two gradients can be reflected by the eigenvalues of its Jacobian matrix. For a 2D dynamical system, suppose  $\lambda_1$  and  $\lambda_2$  are the two eigenvalues of the Jacobian matrix of the system, the fixed point is stable if  $|\lambda_1| < 1$  and  $|\lambda_2| < 1$ , and it is unstable if  $|\lambda_j| > 1$  for  $j = 1$  or  $2$  [38]. The Jacobian matrix  $\mathbf{J}$  of the enhanced Hénon map can be calculated as

$$\mathbf{J} = \begin{vmatrix} \cos(\pi(1 - \tilde{a}x_n^2 + y_n)) \cos(\pi(1 - \tilde{a}x_n^2 + y_n))\pi & \pi(-2\tilde{a}x_n) \\ \pi(-2\tilde{a}x_n) & \cos(\pi\tilde{b}x_n)\pi\tilde{b} \end{vmatrix}. \quad (7)$$

**Table I** shows all the fixed points and related absolute eigenvalues of the Jacobian matrix of the enhanced Hénon map under several parameter settings. One can observe that the enhanced Hénon map has different numbers of fixed points under different parameter settings. For all the fixed points, at least one absolute eigenvalue is larger than one. This means that all these fixed points are unstable.

**Fig. 2(a) and (b)** demonstrates the bifurcation diagrams of the enhanced Hénon map with parameters  $\tilde{a}, \tilde{b} \in [0, 1000]$  and its trajectory under the fixed parameter setting  $(\tilde{a}, \tilde{b}) = (500, 500)$ . As can be observed, the outputs of the enhanced Hénon map distribute in the whole phase plane.

### C. Enhanced 2D-SLM Map

**1) Definition:** When applying 2D-SCS to the 2D-SLM map, i.e., the existing 2D chaotic map,  $\mathbf{F}(x, y)$  in (3) is set as the

**TABLE I**  
FIXED POINTS AND THEIR ABSOLUTE EIGENVALUES OF THE JACOBIAN MATRIX OF THE ENHANCED HÉNON MAP

$(\tilde{a}, \tilde{b})$	Fixed points $(\hat{x}, \hat{y})$	Absolute eigenvalues of $\mathbf{J}_{(\hat{x}, \hat{y})}$	
		$ \lambda_1 $	$ \lambda_2 $
(1, 1)	(-0.4150, -0.9640)	$ \lambda_1  = 3.1295$	$ \lambda_2  = 0.7571$
	(-0.7500, -0.7070)	$ \lambda_1  = 2.1502$	$ \lambda_2  = 2.1502$
	(0, 0)	$ \lambda_1  = 3.1416$	$ \lambda_2  = 3.1416$
	(0.9250, 0.2320)	$ \lambda_1  = 1.9064$	$ \lambda_2  = 1.9064$
	(0.8640, 0.4140)	$ \lambda_1  = 3.8873$	$ \lambda_2  = 1.1606$
(1, 2)	(-0.8040, 0.9440)	$ \lambda_1  = 1.9753$	$ \lambda_2  = 1.9753$
	(-0.5940, 0.5560)	$ \lambda_1  = 5.4248$	$ \lambda_2  = 2.4273$
	(0, 0)	$ \lambda_1  = 4.4429$	$ \lambda_2  = 4.4429$
	(0.4880, 0.0760)	$ \lambda_1  = 5.6949$	$ \lambda_2  = 3.0176$
	(0.5780, -0.4700)	$ \lambda_1  = 3.7709$	$ \lambda_2  = 3.7709$
(2, 1)	(-0.3410, -0.8780)	$ \lambda_1  = 4.9308$	$ \lambda_2  = 0.9015$
	(-0.6750, -0.8530)	$ \lambda_1  = 6.8185$	$ \lambda_2  = 0.5582$
	(0, 0)	$ \lambda_1  = 3.1416$	$ \lambda_2  = 3.1416$
	(0.8020, 0.5830)	$ \lambda_1  = 5.0666$	$ \lambda_2  = 0.9442$
	(0.7180, 0.7760)	$ \lambda_1  = 6.9069$	$ \lambda_2  = 0.6289$
$\vdots$	$\vdots$	$\vdots$	$\vdots$

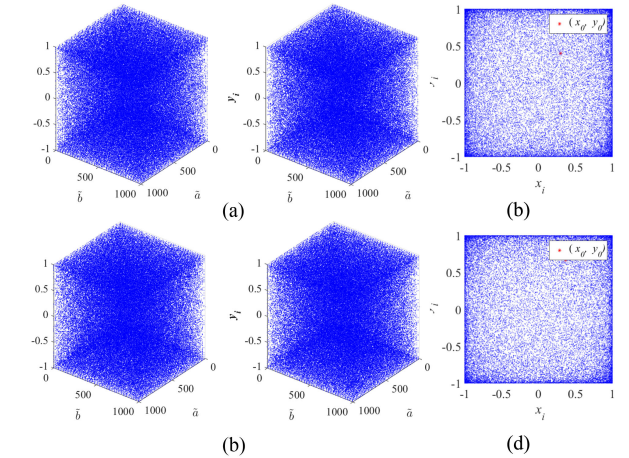


**Fig. 2.** Bifurcation diagrams and trajectories of the (a)-(b) enhanced Hénon, and (c)-(d) enhanced 2D-SLM maps, respectively.

2D-SLM map in (2), the enhanced 2D-SLM map is obtained and it is defined as

$$\begin{cases} x_{n+1} = \sin(\pi\tilde{a}(\sin(\pi y_n) + \tilde{b})x_n(1 - x_n)) \\ y_{n+1} = \sin(\pi\tilde{a}(\sin(\pi x_{n+1}) + \tilde{b})y_n(1 - y_n)) \end{cases} \quad (8)$$

where the two control parameters of the enhanced 2D-SLM map  $\tilde{a}, \tilde{b} \in \mathbb{R}$ .

**2) Stability:** To obtain all the fixed points of the enhanced 2D-SLM map, let  $(x_{n+1}, y_{n+1}) = (x_n, y_n)$ , and the fixed points of the enhanced 2D-SLM map are the solutions of the following

**TABLE II**  
FIXED POINTS AND THEIR ABSOLUTE EIGENVALUES OF THE JACOBIAN MATRIX OF THE ENHANCED 2D-SLM MAP

$(\tilde{a}, \tilde{b})$	Fixed points $(\hat{x}, \hat{y})$	Absolute eigenvalues of $\mathbf{J}_{(\hat{x}, \hat{y})}$
$(1, 1)$	$(-0.2680, -0.7320)$	$ \lambda_1  = 0.1732,  \lambda_2  = 7.1148$
	$(-0.2680, -0.2680)$	$ \lambda_1  = 0.2056,  \lambda_2  = 6.7904$
	$(0.7780, 0.2220)$	$ \lambda_1  = 2.1713,  \lambda_2  = 1.4978$
	$(0.7780, 0.7780)$	$ \lambda_1  = 1.8034,  \lambda_2  = 1.8034$
$(1, 2)$	$(-0.5330, -0.5330)$	$ \lambda_1  = 5.5090,  \lambda_2  = 5.5090$
	$(-0.5330, -0.4680)$	$ \lambda_1  = 6.1328,  \lambda_2  = 3.1040$
	$(0.8460, 0.1540)$	$ \lambda_1  = 3.0448,  \lambda_2  = 2.6760$
	$(0.8460, 0.8460)$	$ \lambda_1  = 2.8545,  \lambda_2  = 2.8545$
$(2, 1)$	$(0.8640, 0.1360)$	$ \lambda_1  = 3.8633,  \lambda_2  = 2.7334$
	$(0.7040, 0.2970)$	$ \lambda_1  = 2.0960,  \lambda_2  = 5.1334$
	$(0.7040, 0.7030)$	$ \lambda_1  = 1.2941,  \lambda_2  = 8.3145$
	$(0.8640, 0.8640)$	$ \lambda_1  = 3.2496,  \lambda_2  = 3.2496$
$\vdots$	$\vdots$	$\vdots$

2D equation:

$$\begin{cases} \hat{x} = \sin(\pi\tilde{a}(\sin(\pi\hat{y}) + \tilde{b}))\hat{x}(1 - \hat{x}) \\ \hat{y} = \sin(\pi\tilde{a}(\sin(\pi\hat{x}) + \tilde{b}))\hat{y}(1 - \hat{y}) \end{cases}. \quad (9)$$

The Jacobian matrix of the enhanced 2D-SLM map is

$$\mathbf{J} = \begin{vmatrix} J_1 & J_2 \\ J_3 & J_4 \end{vmatrix} \quad (10)$$

where

$$\begin{aligned} J_1 &= \cos(M)\pi\tilde{a}(\sin(\pi y_n) + \tilde{b})(1 - 2x_n) \\ J_2 &= \cos(M)\pi\tilde{a}\cos(\pi y_n)\pi x_n(1 - x_n) \\ J_3 &= \cos(N)\pi\tilde{a}y_n(1 - y_n)\cos(\pi \sin(M))\pi J_1 \\ J_4 &= \cos(N)\pi\tilde{a}((\sin(\pi \sin(M)) + \tilde{b})(1 - 2y_n) \\ &\quad + y_n(1 - y_n)\cos(\pi \sin(M))\pi J_2) \\ M &= \pi\tilde{a}(\sin(\pi y_n) + \tilde{b})x_n(1 - x_n) \\ N &= \pi\tilde{a}(\sin(\pi x_{n+1}) + \tilde{b})y_n(1 - y_n). \end{aligned}$$

For the enhanced 2D-SLM map under several parameter settings, **Table II** shows its fixed points and the absolute eigenvalues of its Jacobian matrix at these fixed points. One can observe that the enhanced 2D-SLM map has different numbers of fixed points for different parameters. For each fixed point, at least one absolute eigenvalue is larger than one. This implies that all these fixed points of the enhanced 2D-SLM map are unstable.

**Fig. 2(c) and (d)** shows the bifurcation diagrams of the enhanced 2D-SLM map with parameters  $\tilde{a}, \tilde{b} \in [0, 1000]$ , and its trajectory under the fixed parameter setting  $(\tilde{a}, \tilde{b}) = (500, 500)$ . One can observe that the two variables  $x_n$  and  $y_n$  distribute uniformly within the range  $[-1, 1]$ , indicating that these outputs

can visit all the regions of the phase plane. Thus, the enhanced 2D-SLM map has complex chaotic behaviors from this viewpoint.

The control parameters of the chaotic maps enhanced by 2D-SCS are from existing chaotic maps. Because the employed sine transform in 2D-SCS is a bounded operation for any input, the control parameters of the enhanced Hénon and enhanced 2D-SLM maps can be any large values. When setting their two control parameters  $\tilde{a}$  and  $\tilde{b}$  as different values, the two enhanced chaotic maps can always achieve complex chaotic behaviors. This is verified by their bifurcation diagrams in **Fig. 2** and performance evaluations in Section IV.

#### IV. PERFORMANCE EVALUATION

This section evaluates the performance of the two enhanced chaotic maps of 2D-SCS using the Lyapunov exponent (LE), Kolmogorov entropy (KE), and joint entropy.

##### A. Lyapunov Exponent

The LE describes the average separation rate of two trajectories of a dynamical system beginning from close initial points [39]. It is a widely accepted indicator for the existence of chaos. For the  $n$ -D discrete-time differentiable chaotic map

$$\mathbf{C}(\mathbf{x}) : \begin{cases} x_{n+1}^{(1)} = C_1(x_n^{(1)}, \dots, x_n^{(N)}) \\ \vdots \\ x_{n+1}^{(N)} = C_N(x_n^{(1)}, \dots, x_n^{(N)}) \end{cases}.$$

Its LEs can be calculated as [40]

$$\text{LE}_j = \lim_{t \rightarrow \infty} \frac{1}{t} \ln |\lambda_j| \quad (11)$$

where  $j = 1, 2, \dots, N$ , and  $\lambda_1, \lambda_2, \dots, \lambda_N$  are the  $N$  eigenvalues of the matrix  $\mathbf{J} = \mathbf{J}(\mathbf{x}_1)\mathbf{J}(\mathbf{x}_2) \dots \mathbf{J}(\mathbf{x}_t)$ , where  $\mathbf{J}(\mathbf{x}_n)$  is the Jacobian matrix of  $\mathbf{C}(\mathbf{x})$  at observation time  $n$ . A dynamical system with a positive LE is considered to be chaotic if its phase plane is compacted. A larger positive LE indicates that the close trajectories diverge faster. If a dynamical system has more than one positive LE, its trajectories will separate in several directions. This makes the system achieve hyperchaotic behaviors. The hyperchaotic behavior is more complicated than chaotic behavior.

Our experiments use the toolbox LET<sup>1</sup> to calculate the LEs of different 2D chaotic maps. A 2D chaotic map has two LEs and **Fig. 3** plots the two LEs of the Hénon, 2D-SLM, enhanced Hénon, and enhanced 2D-SLM maps. One can see that the Hénon and 2D-SLM maps have positive LEs in only small parameter ranges. This means that their chaotic ranges are very small. Besides, their chaotic ranges are discontinuous because there exist many periodic windows where the two chaotic maps exhibit regular behaviors. On the other hand, the two enhanced chaotic maps of 2D-SCS have positive LEs in all the parameter ranges and their LEs become larger with the increment of their

<sup>1</sup>[Online]. Available: <https://ww2.mathworks.cn/matlabcentral/fileexchange/233-let?requestedDomain=zh>

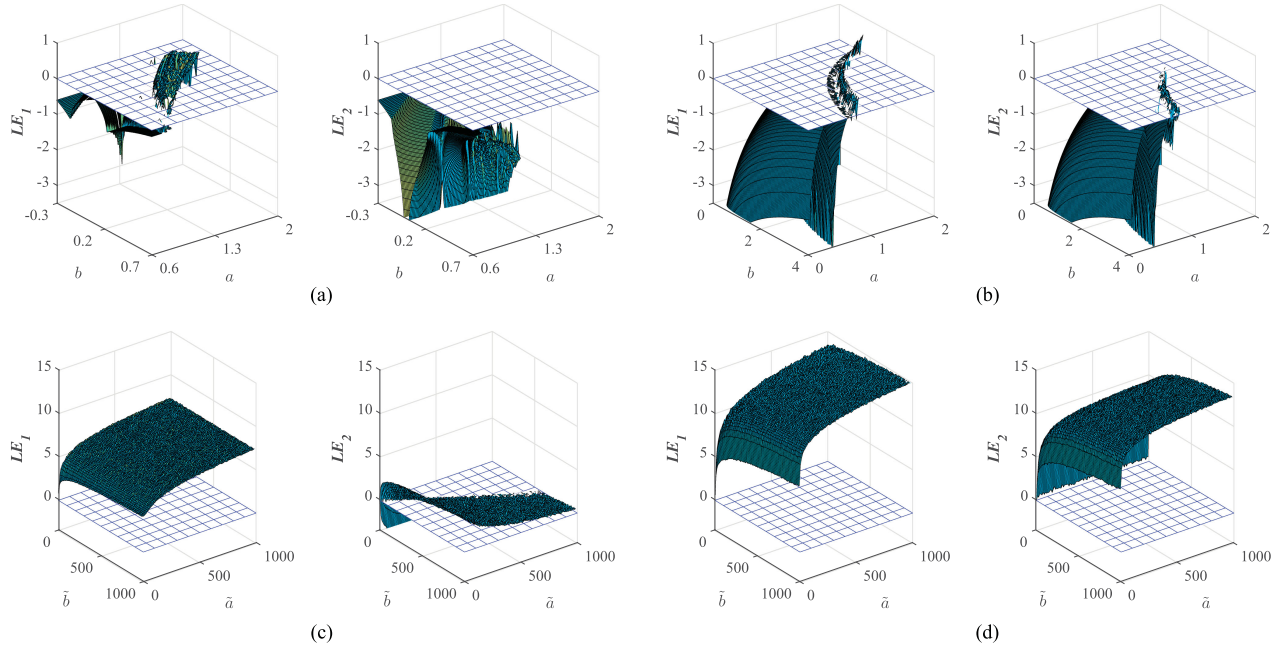


**Fig. 3.** Two LEs of different 2D chaotic maps with the change of their control parameters: (a) Hénon map; (b) 2D-SLM map; (c) enhanced Hénon map; and (d) enhanced 2D-SLM map.

**TABLE III**  
AVERAGE LES AND KES OF SEVERAL 2D AND LATEST 1D CHAOTIC MAPS  
WITHIN THEIR RESPECTIVE CHAOTIC RANGES

Chaotic maps	LE		KE
	LE <sub>1</sub>	LE <sub>2</sub>	
Hénon	0.2764	-2.1035	0.3153
2D-SLM	0.1750	-0.1299	0.3585
SS-SECS [30]		1.7237	1.5940
LS-STBCS [31]		1.3812	1.1276
LS-NCS [41]		0.6919	0.6127
DWSICS [17]		1.7460	0.2172
Enhanced Hénon	6.3766	0.4199	1.9717
Enhanced 2D-SLM	13.1422	11.2536	1.9710

control parameters. They also have two positive LEs in most parameter ranges. This indicates that they have hyperchaotic behaviors in these parameter settings. Notice that the LEs of the two enhanced chaotic maps are plotted only within parameter range [0,1000]. They can obtain positive LEs for any large parameter values.

Table III compares the average LEs of these 2D and several latest 1D chaotic maps within their respective chaotic ranges. These 1D chaotic maps include the sine–sine map in [30] (SS-SECS), logistic-sine map in [31] (LS-STBCS), logistic-sine system in [41] (LS-NCS), and the generated chaotic map in [17] (DWSICS). A 2D chaotic map has two LEs while a 1D chaotic map has only one LE, and the largest LE (LLE) of a chaotic map determines the chaotic behaviors of this chaotic map. One can observe that the two enhanced chaotic maps of 2D-SCS have

considerably larger LLEs than these existing 2D and 1D chaotic maps.

### B. Kolmogorov Entropy

The KE is a type of entropy that can measure the long-term unpredictability of a motion by testing the degree of information loss in the motion [42]. Mathematically, KE is defined as

$$KE = \lim_{\tau \rightarrow 0} \tau^{-1} \lim_{\varepsilon \rightarrow 0} \lim_{m \rightarrow \infty} K_{m,\tau}(\varepsilon) \quad (12)$$

where  $m$  is the embedding dimension, and  $K_{m,\tau}(\varepsilon)$  is defined by

$$K_{m,\tau}(\varepsilon) = - \sum_{i_1, \dots, i_m \leq n(\varepsilon)} P(i_1, \dots, i_m) \log P(i_1, \dots, i_m) \quad (13)$$

where  $P(i_1, \dots, i_m)$  is the joint probability of successfully predicting the orbit in the partition  $\phi_{i_1}$  at unit time  $\tau$ , ..., in the partition  $\phi_{i_m}$  at unit time  $m\tau$ , and  $\phi_{i_1}, \dots, \phi_{i_m}$  represent  $m$  nonoverlapping partitions of a dynamic system's phase plane. A KE value of zero means that a dynamical system has regular behavior and its long-term motion can be estimated. A KE value approaching  $\infty$  means that the long-term motion of a dynamical system is random. A positive KE indicates that a dynamical system has chaotic behavior and its long-term motion has information loss. Thus, the long-term motion of a dynamical system is unpredictable if it has a positive KE and a larger KE indicates faster information loss [42].

Our experiments use the method in [42] to calculate the KEs of different chaotic maps and each calculation uses 12 000 adjacent states truncated from a chaotic signal. Fig. 4 plots the KEs of the Hénon, 2D-SLM, enhanced Hénon, and enhanced 2D-SLM maps. As can be observed, the enhanced Hénon and enhanced

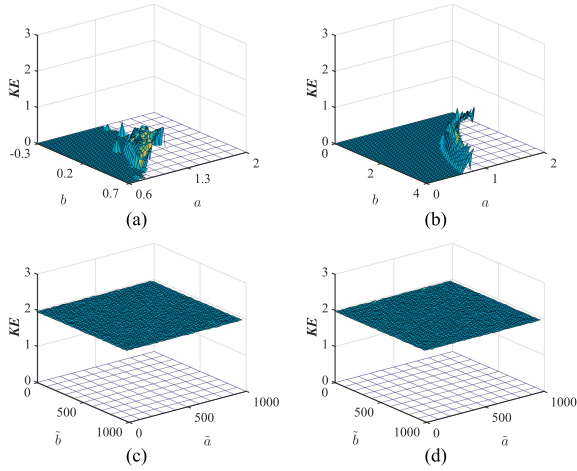


**Fig. 4.** KEs of the time series generated by different 2D chaotic maps: (a) Hénon map; (b) 2D-SLM map; (c) enhanced Hénon map; and (d) enhanced 2D-SLM map.

2D-SLM maps have positive KEs in the entire parameter range, and they have almost the same KEs under different parameter settings. Their KEs are much larger than the KEs of the Hénon and 2D-SLM maps. Besides, Table III presents the average KEs of these 2D chaotic maps and several latest 1D chaotic maps within their respective chaotic ranges. One can observe that the two enhanced chaotic maps of 2D-SCS can achieve considerably larger KEs than other maps. This indicates that the trajectories of these enhanced chaotic maps have better unpredictability.

### C. Joint Entropy

The joint entropy is to test the uncertainty of several signals. Here, it is employed to test the two signals  $X = \{x_1, x_2, \dots, x_n\}$  and  $Y = \{y_1, y_2, \dots, y_n\}$  generated by a 2D chaotic system. Divide the values in  $X$  and  $Y$  into  $N$  states over their discrete probability density function, then the joint entropy of  $X$  and  $Y$  is calculated as

$$H(XY) = - \sum_{i_X=1}^N \sum_{i_Y=1}^N P(b_{i_X} b_{i_Y}) \log_2 P(b_{i_X} b_{i_Y}) \quad (14)$$

where  $b_{i_X}$  and  $b_{i_Y}$  are the  $i_X$ th and  $i_Y$ th states of  $X$  and  $Y$ , and  $P(b_{i_X} b_{i_Y})$  is the joint probability.

The joint entropy  $H(XY)$  is a positive value and its theoretical maximum value can be achieved when  $X$  and  $Y$  are absolutely random and independent from each other, namely  $P(b_i) = 1/N$  and  $P(b_{i_1} b_{i_2}) = P(b_{i_1})P(b_{i_2})$ . Thus, the theoretical  $H(XY)_{\max}$  can be obtained as

$$\begin{aligned} H(XY)_{\max} &= - \sum_{i_X=1}^N \sum_{i_Y=1}^N P(b_{i_X})P(b_{i_Y}) \log_2 (P(b_{i_X})P(b_{i_Y})) \\ &= - \sum_{i_X=1}^N \sum_{i_Y=1}^N (1/N)^2 \log_2 (1/N)^2 \\ &= 2 \log_2 N. \end{aligned} \quad (15)$$

**TABLE IV**  
AVERAGE JOINT ENTROPIES OF THE TWO CHAOTIC SIGNALS  $X$  AND  $Y$  GENERATED BY 2D CHAOTIC MAPS UNDER VARIOUS SIGNAL STATES  $N$

$N$	Hénon	2D-SLM	Enhanced Hénon	Enhanced 2D-SLM
$2^1$	1.6340	1.5659	1.9711	1.9566
$2^2$	2.5088	3.4197	3.8148	3.8159
$2^3$	3.4749	5.0114	5.6848	5.6843
$2^4$	4.5085	6.5900	7.5847	7.5795
$2^5$	5.5602	8.2915	9.5076	9.5017
$2^6$	6.5989	10.0208	11.4513	11.4451
$2^7$	7.6870	11.7877	13.4102	13.4045

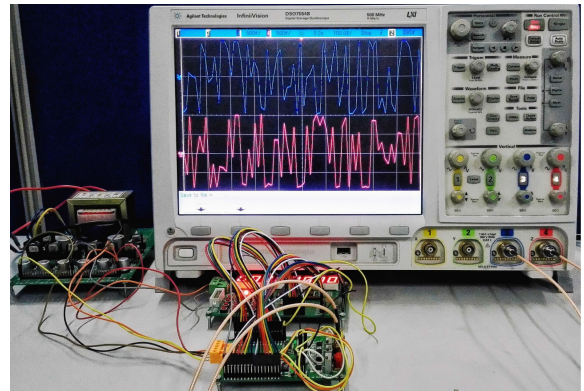


**Fig. 5.** Hardware prototype for the microcontroller-based experiment.

Then, the experimental joint entropy of  $X$  and  $Y$  satisfies that  $0 < H(XY) \leq 2 \log_2 N$  and a larger value indicates more uncertainty of the two signals.

The experiment is set as follows for each 2D chaotic map.

- 1) Randomly select the control parameters from the chaotic ranges.
- 2) Iterate the 2D chaotic map  $2^{3 \times (n+1)}$  times for each signal state  $N \in \{2^1, \dots, 2^n, \dots, 2^7\}$  to generate the chaotic signals  $X$  and  $Y$ .
- 3) Calculate the joint entropies of  $X$  and  $Y$  for each signal state.
- 4) Repeat steps 1)-3) 20 times to obtain the average joint entropies.

Table IV lists the average joint entropies of the Hénon, 2D-SLM, enhanced Hénon, and enhanced 2D-SLM maps under various signal states  $N$ . It shows that the enhanced Hénon and enhanced 2D-SLM maps always have larger joint entropies than the Hénon and 2D-SLM maps under different signal states. This indicates that the two chaotic signals  $X$  and  $Y$  generated by these enhanced chaotic maps have better uncertainty.

## V. HARDWARE IMPLEMENTATION AND APPLICATION

This section investigates the hardware implementation and application of the enhanced Hénon and enhanced 2D-SLM maps of 2D-SCS.

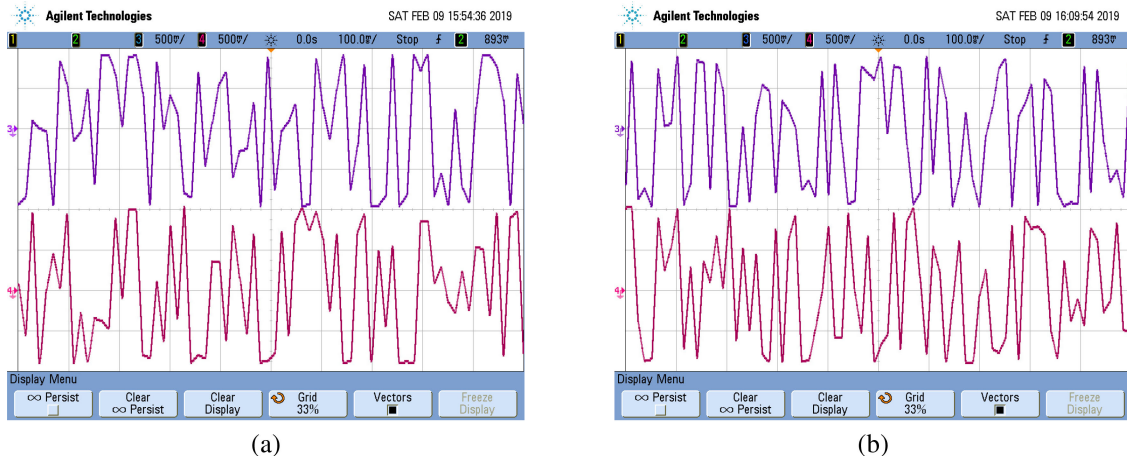


**Fig. 6.** Output time sequences captured from the microcontroller-based experimental platform for the (a) enhanced Hénon and (b) enhanced 2D-SLM maps. The top time sequences are the outputs of  $x_n$  while the bottom time sequences are the outputs of  $y_n$ . The control parameters  $(\tilde{a}, \tilde{b}) = (500, 500)$  and initial values  $(x_0, y_0) = (0.1, 0.1)$ .

#### *A. Hardware Implementation*

When chaotic systems are used in practical applications, they must first be implemented in hardware devices. To show the implementation of 2D-SCS in hardware devices, this section develops a hardware platform to implement the enhanced Hénon and enhanced 2D-SLM maps of 2D-SCS.

**1) Experiment Settings:** As the microcontroller has many advantages, such as small size, simple structure, low cost, and strong controllability, it is widely employed in industrial products. Here, a microcontroller-based platform is developed to implement the enhanced Hénon and enhanced 2D-SLM maps. The hardware devices in this experiment include the ultra-low power microcontroller MSP430F249, 16-bit D/A converter LTC1668, oscilloscope DSO7054B, and other peripheral circuits. The microcontroller is to implement the two enhanced chaotic maps, the D/A converter outputs analog voltage signals, and the oscilloscope displays the analog voltage signals to directly show the implementation results. The experiment is set as follows. First, code the program using C language according to the mathematical models of the enhanced Hénon and enhanced 2D-SLM maps in (5) and (8). Second, download the program to the microcontroller. Finally, run the program in the microcontroller, output the generated analog voltage signals using the D/A converter, and display the signals in the oscilloscope.

**2) Implementation Results:** Fig. 5 shows the hardware prototype for the microcontroller-based platform. In this implementation, the control parameters for the enhanced Hénon and enhanced 2D-SLM maps are set as  $(\tilde{a}, \tilde{b}) = (500, 500)$  and the initial values for the two enhanced chaotic maps are set as  $(x_0, y_0) = (0.1, 0.1)$ . After setting the control parameters and initial values, the experiment platform can generate iterative outputs  $x_n$  and  $y_n$  for the enhanced Hénon and enhanced 2D-SLM maps continuously. To directly show the implementation results, the generated output signals are captured from the oscilloscope and Fig. 6 demonstrates the captured results. One can observe that the two outputs  $x_n$  and  $y_n$  randomly oscillate

in a fixed range, indicating the correctness and feasibility of the implementation of the two enhanced chaotic maps.

### *B. Application in Pseudorandom Number Generator*

Random numbers play an important role in industrial applications such as the industrial simulations, industrial control, and Internet of things [43]–[45]. For example, in the application of Internet of things, random numbers are widely used to develop security schemes for protecting data [44], [45]. Chaotic systems provide a useful tool for designing pseudorandom number generators (PRNGs) because of their properties of initial state sensitivity and unpredictability [46]. This subsection investigates the application of the enhanced chaotic maps of 2D-SCS in PRNG.

**1) Design of Pseudorandom Number Generator:** There are two commonly used strategies when chaotic systems are used to generate pseudorandom numbers. One strategy uses a threshold to determine the random numbers. A random bit 1 is obtained if an output of a chaotic system is larger than the threshold. Otherwise, a random bit 0 is obtained. The other strategy is to directly use a chaotic sequence as random numbers. Our experiment uses the latter strategy to design PRNG, because this strategy can directly reflect the distribution of the chaotic sequences. For a chaotic sequence  $X = \{x_1, x_2, \dots\}$  generated by a chaotic map, transform each value in the sequence into a bit stream according to the IEEE 754 standard, and then directly truncate the 25th–32th bits from the bit stream as pseudorandom numbers. The designed PRNG can be presented as

$$Q_{8(i-1)+1:8i} = \mathbb{N}(x_i)_{25:32} \quad (16)$$

where the function  $\mathbb{N}(\cdot)$  is to transform a value into bit stream following the IEEE 754 standard and  $Q$  is the obtained random number sequence.

**2) Randomness Test:** The TestU01 is a software library to measure the randomness of pseudorandom numbers [47]. It contains a set of predefined test suites. Each test suit is a collection of statistical tests that aim to find out the nonrandomness

**TABLE V**  
USED PARAMETERS FOR ALL THE CHAOTIC MAPS IN THE TESTU01 TEST

Chaotic maps	Parameters
Hénon	$a = 1.36, b = 0.25$
2D-SLM	$a = 0.87, b = 2.86$
SS-SECS [30]	$p = 8.73$
LS-STBCS [31]	$p = 0.98$
LS-NCS [41]	$p = 0.11$
DWSCS [17]	$p = 3.97$
Enhanced Hénon	$\tilde{a} = 736.91, \tilde{b} = 187.67$
Enhanced 2D-SLM	$\tilde{a} = 269.17, \tilde{b} = 23.11$

**TABLE VI**  
TESTU01 TEST RESULTS OF VARIOUS LENGTHS OF BINARY SEQUENCES  
GENERATED BY DIFFERENT CHAOTIC MAPS

Bit Lengths	$2^{18}$ bits	$2^{24}$ bits	$2^{30}$ bits
<i>Rabbit</i>			
Hénon	33/33	39/39	38/40
2D-SLM	33/33	39/39	39/40
SS-SECS [30]	33/33	34/39	7/40
LS-STBCS [31]	33/33	36/39	30/40
LS-NCS [41]	32/33	36/39	31/40
DWSCS [17]	33/33	37/39	20/40
Enhanced Hénon	33/33	39/39	40/40
Enhanced 2D-SLM	33/33	39/39	40/40
<i>Alphabit</i>			
Hénon	17/17	17/17	17/17
2D-SLM	17/17	17/17	17/17
SS-SECS [30]	17/17	14/17	0/17
LS-STBCS [31]	17/17	17/17	10/17
LS-NCS [41]	17/17	17/17	13/17
DWSCS [17]	17/17	17/17	0/17
Enhanced Hénon	17/17	17/17	17/17
Enhanced 2D-SLM	17/17	17/17	17/17
<i>BlockAlphabit</i>			
Hénon	102/102	102/102	102/102
2D-SLM	102/102	102/102	102/102
SS-SECS [30]	102/102	83/102	0/102
LS-STBCS [31]	102/102	102/102	61/102
LS-NCS [41]	102/102	102/102	93/102
DWSCS [17]	102/102	102/102	42/102
Enhanced Hénon	102/102	102/102	102/102
Enhanced 2D-SLM	102/102	102/102	102/102

$p/q$  indicates passing  $p$  out of  $q$  statistical tests.

areas from different aspects. Among all the predefined test suits in TestU01, the *Rabbit*, *Alphabit*, and *BlockAlphabit* test suits were developed for binary sequences and are used in our experiments. The test binary sequences are of lengths  $2^{18}$ ,  $2^{24}$ , and  $2^{30}$  bits. For different lengths of binary sequences, the *Alphabit* and *BlockAlphabit* test suits apply 17 and 102 statistical tests, respectively. For binary sequences with lengths  $2^{18}$ ,  $2^{24}$ , and  $2^{30}$  bits, the *Rabbit* test suit applies 33, 39, and 40 statistical tests, respectively.

To obtain more neutral test results, an open-source software version<sup>2</sup> is used to test the randomness of the pseudorandom numbers generated by different chaotic maps. The initial values for all the 2D chaotic maps are set as  $(x_0, y_0) = (0.1, 0.1)$  and that for all the 1D chaotic maps are set as  $x_0 = 0.1$ . The control parameters are randomly selected from their respective chaotic ranges and Table V lists these selected control parameters for all the chaotic maps. Table VI shows the TestU01 test results for these chaotic maps with different lengths of binary sequences. One can observe that when the length of the binary sequence is  $2^{18}$  bits, almost all the chaotic maps can pass all the statistical tests in the three test suits. When the length of the binary sequence increases to  $2^{30}$  bits, only the two enhanced chaotic maps of 2D-SCS can pass all the statistical tests in the three test suits. Although the binary sequences generated by the Hénon and 2D-SLM maps fail only a few statistical tests, this means that there exist nonrandomness areas in some aspects. Thus, only the two enhanced chaotic maps of 2D-SCS can pass the TestU01 test. The existing 2D and several latest 1D chaotic maps cannot pass the test. This verifies the effectiveness of the proposed 2D-SCS in generating pseudorandom numbers. Because many authentication schemes require random numbers [48], [49], the enhanced chaotic maps of 2D-SCS can be integrated into these authentication schemes.

## VI. CONCLUSION

This paper first studied the drawbacks of existing 2D chaotic maps. To address these drawbacks, this paper proposed a 2D-SCS to enhance the chaos complexity of 2D chaotic map. 2D-SCS uses a sine transform as a chaotification framework and applies it to each output of existing chaotic maps. Two cases of enhanced chaotic maps were studied to demonstrate the effectiveness of 2D-SCS. Performance analysis showed that the chaotic maps enhanced by 2D-SCS have more complex chaotic behaviors and considerably larger chaotic ranges than existing 2D chaotic maps. A microcontroller-based hardware platform was developed to show the hardware implementation of the enhanced chaotic maps of 2D-SCS. To demonstrate the application of 2D-SCS, the two enhanced chaotic maps of 2D-SCS are investigated in designing PRNG. Performance analysis showed that these enhanced chaotic maps can generate better random numbers than two existing 2D and several latest 1D chaotic maps.

## ACKNOWLEDGMENT

The authors would like to sincerely thank the anonymous reviewers for their valuable comments and suggestions that greatly contributed to improving the quality of the manuscript.

## REFERENCES

- [1] Z. Wang and D. Liu, "A data-based state feedback control method for a class of nonlinear systems," *IEEE Trans. Ind. Inform.*, vol. 9, no. 4, pp. 2284–2292, Apr. 2013.
- [2] X. Meng, P. Rozycski, J.-F. Qiao, and B. M. Wilamowski, "Nonlinear system modeling using RBF networks for industrial application," *IEEE Trans. Ind. Inform.*, vol. 14, no. 3, pp. 931–940, Mar. 2018.

<sup>2</sup>[Online]. Available: <http://simul.iro.umontreal.ca/testu01/tu01.html>

- [3] Y. Deng, H. Hu, W. Xiong, N. N. Xiong, and L. Liu, "Analysis and design of digital chaotic systems with desirable performance via feedback control," *IEEE Trans. Syst., Man, Cybern., Syst.*, vol. 45, no. 8, pp. 1187–1200, Aug. 2015.
- [4] W. Sun, Y. Liu, and H. Gao, "Constrained sampled-data ARC for a class of cascaded nonlinear systems with applications to motor-servo systems," *IEEE Trans. Ind. Inform.*, vol. 15, no. 2, pp. 766–776, Feb. 2019.
- [5] C. Li, B. Feng, S. Li, J. Kurths, and G. Chen, "Dynamic analysis of digital chaotic maps via state-mapping networks," *IEEE Trans. Circuits Syst. I*, vol. 66, no. 6, pp. 2322–2335, Jun. 2019.
- [6] Q. Wang *et al.*, "Theoretical design and FPGA-based implementation of higher-dimensional digital chaotic systems," *IEEE Trans. Circuits Syst. I*, vol. 63, no. 3, pp. 401–412, Mar. 2016.
- [7] H. G. Schuster and W. Just, *Deterministic Chaos: An Introduction*. Hoboken, NJ, USA: Wiley, 2006.
- [8] R. L. Devaney, *An Introduction to Chaotic Dynamical Systems*, 2nd ed. Boulder, CO, USA: Westview, 2003.
- [9] D. Abbasinezhad-Mood and M. Nikooghadam, "Efficient anonymous password-authenticated key exchange protocol to read isolated smart meters by utilization of extended Chebyshev chaotic maps," *IEEE Trans. Ind. Inform.*, vol. 14, no. 11, pp. 4815–4828, Nov. 2018.
- [10] C. Li, D. Lin, B. Feng, J. Lü, and F. Hao, "Cryptanalysis of a chaotic image encryption algorithm based on information entropy," *IEEE Access*, vol. 6, pp. 75834–75842, 2018.
- [11] D. Chen, "Research on traffic flow prediction in the big data environment based on the improved RBF neural network," *IEEE Trans. Ind. Inform.*, vol. 13, no. 4, pp. 2000–2008, 2017.
- [12] P. Chittora, A. Singh, and M. Singh, "Chebyshev functional expansion based artificial neural network controller for shunt compensation," *IEEE Trans. Ind. Inform.*, vol. 14, no. 9, pp. 3792–3800, Sep. 2018.
- [13] S.-L. Chen *et al.*, "Randomness enhancement using digitalized modified logistic map," *IEEE Trans. Circuits Syst. II, Exp. Briefs*, vol. 57, no. 12, pp. 996–1000, Dec. 2010.
- [14] Z. Hua, B. Zhou, and Y. Zhou, "Sine chaotification model for enhancing chaos and its hardware implementation," *IEEE Trans. Ind. Electron.*, vol. 66, no. 2, pp. 1273–1284, Feb. 2019.
- [15] M. Bakiri, C. Guyeux, J.-F. Couchot, L. Marangio, and S. Galatolo, "A hardware and secure pseudorandom generator for constrained devices," *IEEE Trans. Ind. Inform.*, vol. 14, no. 8, pp. 3754–3765, 2018.
- [16] S. Vaidyanathan and C. Volos, *Advances and Applications in Chaotic Systems*. Berlin, Germany: Springer, 2016.
- [17] Y. Wu, Y. Zhou, and L. Bao, "Discrete wheel-switching chaotic system and applications," *IEEE Trans. Circuits Syst. I*, vol. 61, no. 12, pp. 3469–3477, Dec. 2014.
- [18] E. Zeraoulia, *Robust Chaos and Its Applications*, vol. 79. Singapore: World Scientific, 2012.
- [19] M. Liu, S. Zhang, Z. Fan, and M. Qiu, " $H_\infty$  state estimation for discrete-time chaotic systems based on a unified model," *IEEE Trans. Syst., Man, Cybern. B*, vol. 42, no. 4, pp. 1053–1063, Aug. 2012.
- [20] S. Sivakumar and S. Sivakumar, "Marginally stable triangular recurrent neural network architecture for time series prediction," *IEEE Trans. Cybern.*, vol. 48, no. 10, pp. 2836–2850, Oct. 2018.
- [21] A. Miranian and M. Abdollahzade, "Developing a local least-squares support vector machines-based neuro-fuzzy model for nonlinear and chaotic time series prediction," *IEEE Trans. Neural Netw. Learn. Syst.*, vol. 24, no. 2, pp. 207–218, Feb. 2013.
- [22] S. Ergün, "On the security of chaos based true random number generators," *IEICE Trans. Fundam. Electron., Commun. Comput. Sci.*, vol. 99, no. 1, pp. 363–369, 2016.
- [23] Y. Deng, H. Hu, N. N. Xiong, W. Xiong, and L. Liu, "A general hybrid model for chaos robust synchronization and degradation reduction," *Inf. Sci.*, vol. 305, pp. 146–164, 2015.
- [24] Z. Hua, Y. Zhou, and H. Huang, "Cosine-transform-based chaotic system for image encryption," *Inf. Sci.*, vol. 480, pp. 403–419, 2019.
- [25] C.-Y. Li, Y.-H. Chen, T.-Y. Chang, L.-Y. Deng, and K. To, "Period extension and randomness enhancement using high-throughput reseeding-mixing PRNG," *IEEE Trans. Very Large Scale Integr. (VLSI) Syst.*, vol. 20, no. 2, pp. 385–389, Feb. 2012.
- [26] H. Hu, Y. Xu, and Z. Zhu, "A method of improving the properties of digital chaotic system," *Chaos, Solitons Fractals*, vol. 38, no. 2, pp. 439–446, 2008.
- [27] L. Liu, J. Lin, S. Miao, and B. Liu, "A double perturbation method for reducing dynamical degradation of the digital baker map," *Int. J. Bifurcation Chaos*, vol. 27, no. 7, 2017, Art. no. 1750103.
- [28] R. Lan, J. He, S. Wang, Y. Liu, and X. Luo, "A parameter-selection-based chaotic system," *IEEE Trans. Circuits Syst. II*, vol. 66, no. 3, pp. 492–496, Mar. 2019.
- [29] Y.-W. Wang and Z.-H. Guan, "Generalized synchronization of continuous chaotic system," *Chaos, Solitons Fractals*, vol. 27, no. 1, pp. 97–101, 2006.
- [30] C. Pak and L. Huang, "A new color image encryption using combination of the 1D chaotic map," *Signal Process.*, vol. 138, pp. 129–137, 2017.
- [31] Z. Hua, B. Zhou, and Y. Zhou, "Sine-transform-based chaotic system with FPGA implementation," *IEEE Trans. Ind. Electron.*, vol. 65, no. 3, pp. 2557–2566, Mar. 2018.
- [32] Z. Hua, Y. Zhou, C.-M. Pun, and C. L. P. Chen, "2D sine logistic modulation map for image encryption," *Inf. Sci.*, vol. 297, pp. 80–94, 2015.
- [33] R. Zhang and S. Yang, "Robust chaos synchronization of fractional-order chaotic systems with unknown parameters and uncertain perturbations," *Nonlinear Dyn.*, vol. 69, no. 3, pp. 983–992, 2012.
- [34] S. Chen, S. Yu, J. Lü, G. Chen, and J. He, "Design and FPGA-based realization of a chaotic secure video communication system," *IEEE Trans. Circuits Syst. Video Technol.*, vol. 28, no. 9, pp. 2359–2371, Sep. 2018.
- [35] S. Yu, J. Lü, and G. Chen, "Theoretical design and circuit implementation of multidirectional multi-torus chaotic attractors," *IEEE Trans. Circuits Syst. I*, vol. 54, no. 9, pp. 2087–2098, 2007.
- [36] S. Yu, J. Lü, G. Chen, and X. Yu, "Generating grid multiwing chaotic attractors by constructing heteroclinic loops into switching systems," *IEEE Trans. Circuits Syst. II, Exp. Briefs*, vol. 58, no. 5, pp. 314–318, May 2011.
- [37] Z. Hua and Y. Zhou, "Dynamic parameter-control chaotic system," *IEEE Trans. Cybern.*, vol. 46, no. 12, pp. 3330–3341, Dec. 2016.
- [38] Z. Elhadj and J. Sprott, "On the dynamics of a new simple 2-D rational discrete mapping," *Int. J. Bifurcation Chaos*, vol. 21, no. 1, pp. 155–160, 2011.
- [39] A. Wolf, J. B. Swift, H. L. Swinney, and J. A. Vastano, "Determining Lyapunov exponents from a time series," *Physica D, Nonlinear Phenomena*, vol. 16, no. 3, pp. 285–317, 1985.
- [40] G.-C. Wu and D. Baleanu, "Jacobian matrix algorithm for Lyapunov exponents of the discrete fractional maps," *Commun. Nonlinear Sci. Numer. Simul.*, vol. 22, no. 1/3, pp. 95–100, 2015.
- [41] Y. Zhou, L. Bao, and C. L. P. Chen, "A new 1D chaotic system for image encryption," *Signal Process.*, vol. 97, pp. 172–182, 2014.
- [42] P. Grassberger and I. Procaccia, "Estimation of the Kolmogorov entropy from a chaotic signal," *Phys. Rev. A*, vol. 28, no. 4, pp. 2591–2593, 1983.
- [43] H. Martin, P. Peris-Lopez, J. E. Tapiador, and E. San Millan, "A new TRNG based on coherent sampling with self-timed rings," *IEEE Trans. Ind. Inform.*, vol. 12, no. 1, pp. 91–100, Jan. 2016.
- [44] Y. Zhao, L. T. Yang, and J. Sun, "A secure high-order CFS algorithm on clouds for industrial Internet of things," *IEEE Trans. Ind. Inform.*, vol. 14, no. 8, pp. 3766–3774, Aug. 2018.
- [45] M. Ma, D. He, N. Kumar, K.-K. R. Choo, and J. Chen, "Certificateless searchable public key encryption scheme for industrial Internet of things," *IEEE Trans. Ind. Inform.*, vol. 14, no. 2, pp. 759–767, Feb. 2018.
- [46] S. H. Strogatz, *Nonlinear Dynamics and Chaos: With Applications to Physics, Biology, Chemistry, and Engineering*, 1st ed. Boulder, CO, USA: Westview, 2001.
- [47] P. L'Ecuyer and R. Simard, "TestU01: A C library for empirical testing of random number generators," *ACM Trans. Math. Softw.*, vol. 33, no. 4, 2007, Art. no. 22.
- [48] S. Roy, S. Chatterjee, A. K. Das, S. Chattopadhyay, S. Kumari, and M. Jo, "Chaotic map-based anonymous user authentication scheme with user biometrics and fuzzy extractor for crowdsourcing Internet of things," *IEEE Internet Things J.*, vol. 5, no. 4, pp. 2884–2895, Aug. 2018.
- [49] Q. Jiang, F. Wei, S. Fu, J. Ma, G. Li, and A. Alelaiwi, "Robust extended chaotic maps-based three-factor authentication scheme preserving biometric template privacy," *Nonlinear Dyn.*, vol. 83, no. 4, pp. 2085–2101, 2016.



**Zhongyun Hua** (S'14–M'16) received the B.S. degree from Chongqing University, Chongqing, China, in 2011, and the M.S. and Ph.D. degrees from the University of Macau, Macau, China, in 2013 and 2016, respectively, all in software engineering.

He is currently an Associate Professor with the Department of Computer Science and Technology, Harbin Institute of Technology, Shenzhen, China. His research interests include chaotic system, chaos-based applications, and

multimedia security.



**Yicong Zhou** (M'07–SM'14) received the B.S. degree from Hunan University, Changsha, China, in 1992, and the M.S. and Ph.D. degrees from Tufts University, Massachusetts, MA, USA, in 2008 and 2010, respectively, all in electrical engineering.

He is an Associate Professor and Director of the Vision and Image Processing Laboratory, Department of Computer and Information Science, University of Macau, Macau, China.

His research interests include chaotic systems, multimedia security, computer vision, and machine learning.

Dr. Zhou is an Associate Editor for the IEEE TRANSACTIONS ON CIRCUITS AND SYSTEMS FOR VIDEO TECHNOLOGY, IEEE TRANSACTIONS ON GEOSCIENCE AND REMOTE SENSING, and several other journals. He is a Senior Member of the International Society for Optical Engineering (SPIE). He is a Co-Chair of the Technical Committee on Cognitive Computing in the IEEE Systems, Man, and Cybernetics Society. He was a recipient of the Third Price of Macau Natural Science Award in 2014.



**Bocheng Bao** received the B.S. and M.S. degrees in electronic engineering from the University of Electronics Science and Technology of China, Chengdu, China, in 1986 and 1989, respectively, and the Ph.D. degree in information and communication engineering, from Nanjing University of Science and Technology, Nanjing, China, in 2010.

He has more than 20 years experience in the industry and was with several enterprises as Senior Engineer and General Manager. From 2008 to 2011, he was a Professor with the School of Electrical and Information Engineering, Jiangsu University of Technology, Changzhou, China. Then, he was a Full Professor with the School of Information Science and Engineering, Changzhou University, Changzhou, China. From 2013, he visited the Department of Electrical and Computer Engineering, University of Calgary, Calgary, AB, Canada. He has authored three academic monographs and more than 160 journal papers, including two hot papers, and 13 highly cited papers. His research interests include bifurcation and chaos, analysis and simulation in neuromorphic circuits, power electronic circuits, and nonlinear circuits and systems.

Dr. Bao was the recipient of The IET Premium Awards in 2018.